

R3, an Accurate JFET and 3-Terminal Diffused Resistor Model

Colin C. McAndrew

Motorola, Tempe, AZ, Colin.McAndrew@motorola.com

ABSTRACT

This paper presents an improved compact model for diffused resistors and JFETs, valid over geometry, bias, and temperature. The model includes a physically based junction depletion model, a new and accurate velocity saturation model derived from data, and self-heating, which is important for low sheet resistance devices.

Keywords: JFET, diffused resistor, SPICE model, compact model, velocity saturation.

1 INTRODUCTION

As we all know from introductory classes in physics and engineering, Ohm's law tells us that $V = IR$ for a resistor. So for IC simulation and design we can take that as given, and concentrate on modeling "real" devices like MOSFETs and BJTs, right? Wrong!

Real resistors do not have linear $I(V)$ characteristics, but deviate from this because of depletion pinching (for diffused resistors, which are JFETs), velocity saturation, self-heating, and Schottky effects and self-heating at contacts. For example, the effective mobility degradation with bias due to self-heating is [1]

$$R/R_0 = \mu_{red} = 1 + \frac{R_{THA}T_{C1}}{\rho_s} \left(\frac{V}{L}\right)^2 \quad (1)$$

where R_{THA} is the thermal resistance per unit area, and the other terms have their usual meaning. Self-heating is thus important for short resistors in low sheet resistance layers.

The details of resistor nonlinearities can be important for whether a circuit meets or fails specifications, especially where harmonic distortion is a key performance metric, and this depends on the linearity (or otherwise) of resistors. So accurate modeling of the nonlinear $I(V)$ characteristics is critical for some analog and mixed-signal applications.

This paper presents a physically-based compact model for diffused resistors and JFETs. The standard SPICE JFET model does not model depletion pinching accurately, and does not include velocity saturation or self-heating. A significantly improved model was presented in [2]; however, this model does not include self-heating, has only a simple velocity saturation model that does not accurately represent measured data, and has only an empirical approach for pinch-off voltage calculation.

This paper presents a diffused resistor and JFET model based on [2] that is significantly more accurate as it overcomes the deficiencies listed above. It also simplifies the basic depletion pinching formulation of [2], yet retains the same accuracy over geometry. The two section resistance model and 1/6:2/3:1/6 capacitance partitioning of [2] has proved accurate to date, so the formulation presented here is for a single section DC model and assumes implementation is a sectional model like [2].

2 DEPLETION MODEL

Fig. 1 shows a cross section of a diffused resistor.

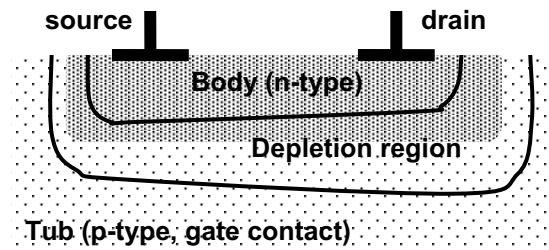


Fig. 1 Diffused Resistor Cross Section

The analysis of [2] gives a resistor current in the presence of depletion pinching, but not velocity saturation, as

$$I = \frac{q\mu_0 N x_0 W}{L} \left(1 - a\sqrt{\psi_a + \bar{V}}\right) \left(1 - \frac{b}{W}\sqrt{\psi_p + \bar{V}}\right) V_{ds} \quad (2)$$

where W and L are the effective width and length, N and x_0 are the doping and depth of the resistor body, ψ_a and ψ_p are the built-in potentials of the bottom (area) and side-wall (perimeter) junctions, a and b are depletion width factors for the bottom and side-wall, and the average body to tub (gate) bias is $\bar{V} = 0.5(V_{dg} + V_{sg})$. For resistors commonly used in IC processes the bias dependence of the last two terms in (2) is relatively small, and $\psi_a \approx \psi_p$, so expanding the product of the depletion pinching terms in (2) and dropping small terms gives a good approximation

$$I_{depl} = G_F \left(1 - D_F \sqrt{P + \bar{V}}\right) V_{ds} \quad (3)$$

where $D_F = D_a + D_p/W$ is an effective depletion factor, $P = 0.5(\psi_a + \psi_p)$, and the effective conductance factor is $G_F = 1/(R_0(1 - D\sqrt{P}))$ where R_0 is the zero bias resistance.

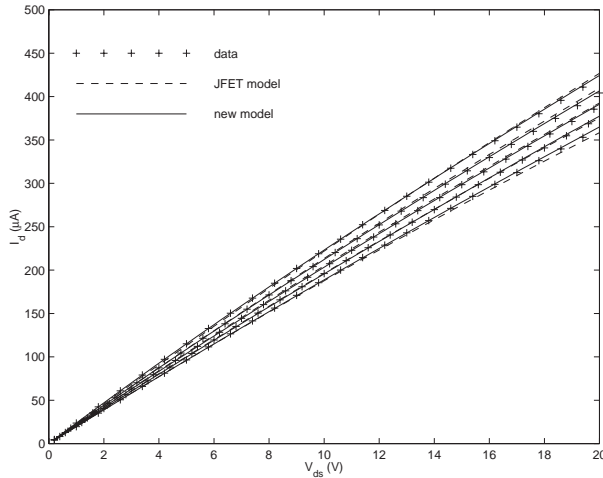


Fig. 2 $I_d(V_{ds}, V_{sg})$ for a wide, long resistor.

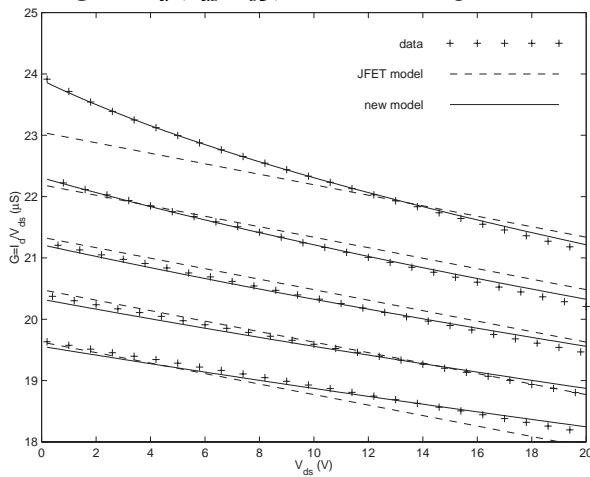


Fig. 3 $G(V_{ds}, V_{sg})$ for a wide, long resistor.

Fig. 2 and Fig. 3 show current and conductance $G = I_d / V_{ds}$ (for a long resistor, so velocity saturation and self-heating are negligible) from data, the model (3), and the SPICE JFET model $I_d = \beta V_{ds} (2(V_{gs} - V_{TO}) - V_{ds})$. The model (3) agrees well with the measured data, the SPICE JFET model does not exhibit even the correct qualitative nonlinear behavior with bias. The nonlinear “depletion” nature of the bias dependence is clear in the data of Fig. 3 and in the model (3), whereas the bias dependence of G is linear with bias for the JFET model. The RMS and maximum errors for the JFET model are 0.89% and 3.7%, respectively, and for the model (3) are 0.25% and 0.59%, respectively.

In practice, to allow greater flexibility in modeling the geometry dependence of the depletion pinching effect, the effective depletion pinching factor is modeling as

$$D_F = D_{F\infty} + D_{FW} / W + D_{FL} / L + D_{FWL} / WL \quad (4)$$

and by use of a selector the geometries used to calculate the depletion factor can be either design dimensions or effective electrical dimensions. The latter can be more

accurate, but the former can be simpler to characterize. The effective width models used are those of [3].

3 VELOCITY SATURATION

Besides modeling the depletion pinching effect, accurate modeling of the nonlinearity of highly linear resistors requires accurate modeling of velocity saturation. Velocity saturation is thought of as only being important to model short devices. However, its effect on nonlinearity is important even for “long” devices.

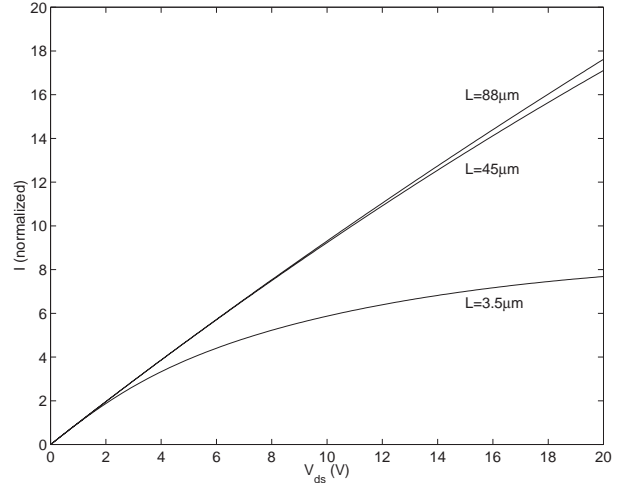


Fig. 4 Normalized $I(V)$ data with velocity saturation.

Fig. 4 shows data from high sheet resistance (so self-heating is negligible) p -type resistors, normalized by low low-field conductance. From (3) the depletion pinching is independent of L so the differences between the curves are primarily from velocity saturation. The effect is noticeable at $L = 45 \mu\text{m}$, and although it looks to be small, it is the difference with respect to a perfectly linear $I(V)$ relation that is important for distortion, and for this purpose the effect is significant.

Rather than analyzing velocity saturation as a velocity versus electric field relation, $v(E)$, a simple and useful way to study the effect is in a reciprocal sense, as an effective mobility reduction factor,

$$\mu_{red}(E) = \mu_0 / \mu(E). \quad (5)$$

The two commonest models for μ_{red} are [4], [5]

$$\mu_{red}(V) = 1 + \frac{\mu_0 |V|}{v_{sat} L}, \quad \mu_{red}(V) = \sqrt{1 + \left(\frac{\mu_0 |V|}{v_{sat} L} \right)^2} \quad (6)$$

where the symbols have their conventional meaning. The first form is often used for analytic simplicity, the second for improved accuracy and lack of a singularity at $V = 0$. Although both forms exhibit qualitatively the correct behavior, they are not accurate for distortion modeling.

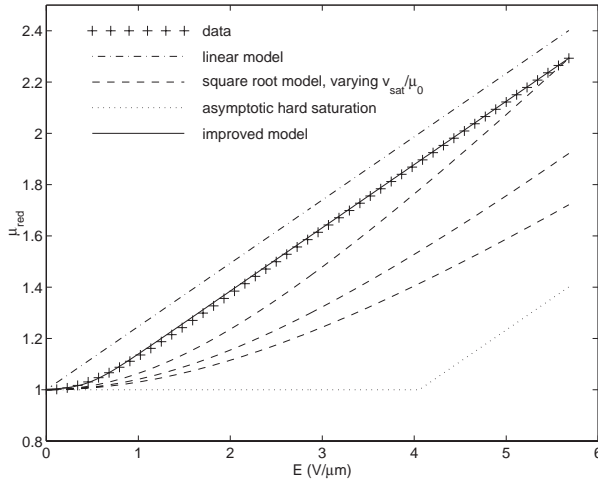


Fig. 5 Mobility degradation due to velocity saturation.

Fig. 5 shows μ_{red} calculated from measured data, with the models (6). The square root model has the critical field $E_{cr} = v_{sat} / \mu_0$ calculated in 3 ways: to match the value of μ_{red} at the highest measured field; to match the slope of $\mu_{red}(E)$ at the highest measured field; and to match the asymptotic slope as $E \rightarrow \infty$. The inaccuracy in the models (6) is clear (the linear model is used in [2]).

Note that for small fields the square root model is

$$\mu_{red}(V) \approx 1 + \frac{\mu_0^2}{2v_{sat}^2} \left(\frac{V}{L} \right)^2 \quad (7)$$

which has the same form as (1). The effects of velocity saturation and self-heating are similar for low bias DC operation (they are qualitatively different for high bias DC operation and AC operation).

The measured μ_{red} data have the following characteristics. Value 1 at $E = 0$, symmetry with respect to E , asymptotically approaches $1 + (E - E_{co})/E_{cr}$ for large E where E_{co} is a corner field, and value $1 + \delta$ at E_{co} . An empirical model that has these characteristics is

$$\mu_{red} = 1 + \sqrt{\left(\frac{E - E_{ce}}{2E_{cr}} \right)^2 + U} + \sqrt{\left(\frac{E + E_{ce}}{2E_{cr}} \right)^2 + U} - \frac{E_{co}}{E_{cr}} \quad (8)$$

where $U = d\mu E_{ce} / E_{cr}$, $d\mu$ is a fitting parameter for the ‘‘hardness’’ of the corner at E_{co} ($d\mu \approx \delta^2 E_{cr} / E_{ce}$), and an effective corner field

$$E_{ce} = \sqrt{E_{co}^2 + (2d\mu E_{cr})^2} - 2d\mu E_{cr} \quad (9)$$

is used to ensure that the asymptote for large E is correct. Fig. 6 shows how the model is parameterized, initial parameter values are calculated from $\mu_{red}(E)$ characteristics and then refined using optimization.

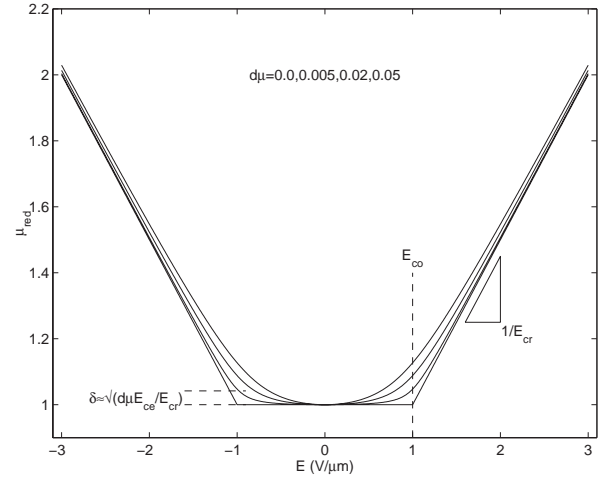


Fig. 6 Velocity saturation model characteristics.

The current in the improved model is

$$I_{ds} = I_{depl} / \mu_{red} \quad (10)$$

where I_{depl} is from (2) and μ_{red} is from (8).

4 SATURATION VOLTAGE

The drain end of a resistor pinches off when the mobile carrier density there is zero, i.e. when V_{dg} is

$$V_P = 1 / D_F^2 - P. \quad (11)$$

This was the basic definition used in [2]. However, because of approximations made during derivation of (1) the small-signal conductance $g_d = \partial I_d / \partial V_d$ is negative at V_P . A better definition of saturation is when $g_d = 0$. For (2)

$$V_{sat} = \frac{1 - 3D_F^2(P + V_{sg}) + \sqrt{1 + 3D_F^2(P + V_{sg})}}{9D_F^2/4}. \quad (12)$$

However, this does not take velocity saturation into account. For a general velocity saturation model applied on top of an existing model, as in (10), it is not possible to guarantee that a closed form solution for the V_{ds} at which $g_d = 0$. Indeed, there is no closed form solution for $g_d = 0$ for the models (2) and (8). The potential problem with an approximate solution is that if this value is greater than the actual value at which $g_d = 0$ then the model exhibits a negative output conductance glitch, which is highly undesirable.

Fortunately, and somewhat counter-intuitively, if a μ_{red} model that is less than the true value is used (actually that has a greater $(1/\mu_{red}) \partial \mu_{red} / \partial E$), then this gives a calculated saturation voltage that is guaranteed to be less than the actual value where $g_d = 0$, hence guaranteeing that there is not negative output conductance glitch.

V_{sat} is therefore calculated as the value of V_{ds} at which the derivative of

$$I = \frac{G_F \left(1 - D_F \sqrt{P + \bar{V}}\right) V_{ds}}{1 + (V_{ds}/L - E_{co})/E_{cr}} \quad (13)$$

is zero. This gives a fourth order equation that has an analytic solution. For low field velocity saturation is not important and the underestimation of V_{sat} is small. For high field the simple model $1 + (E - E_{co})/E_{cr}$ is very close to the more accurate model (8) and so the accuracy is again good. V_{ds} is limited to V_{sat} via the limiting function

$$V = \frac{2V_{ds}V_{sat}}{\sqrt{(V_{ds} - V_{sat})^2 + 4A^2} + \sqrt{(V_{ds} + V_{sat})^2 + 4A^2}} \quad (14)$$

which maintains symmetry.

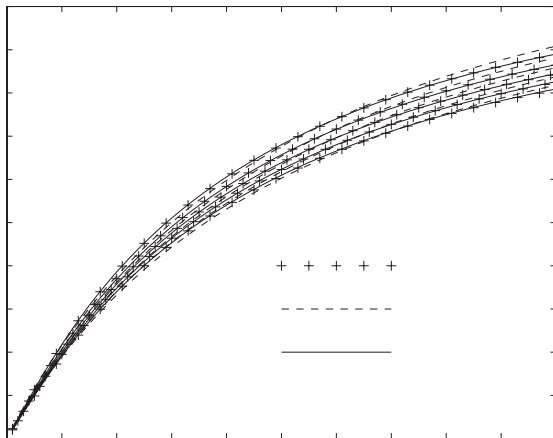


Fig. 7 $I_d(V_{ds}, V_{sg})$ for a wide, short resistor.

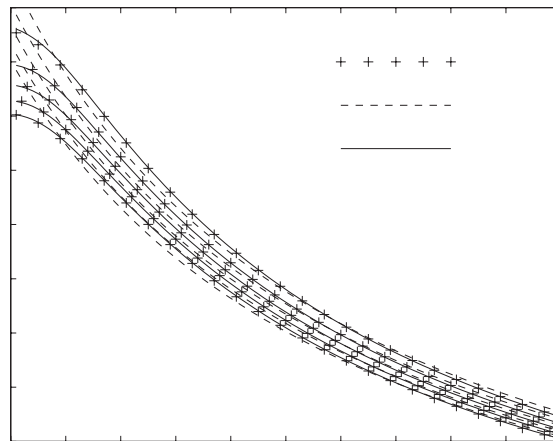


Fig. 8 $G(V_{ds}, V_{sg})$ for a wide, short resistor.

Fig. 7 and Fig. 8 show current and $G = I_d/V_{ds}$ for a wide, short resistor. Also shown are the model (13) and the depletion pinching model (2) with the linear model for mobility reduction due to velocity saturation in (6). The improved accuracy of the velocity saturation model (8) is clear. In particular, the simple linear velocity saturation model of (6), apart from having a singularity at zero, is inaccurate and qualitatively incorrect near zero.

5 CONCLUSIONS

An improved model for diffused resistors and JFETs has been presented. The model improves on that of [2] by having a simpler formulation, having a more accurate velocity saturation model, and having an accurate and analytic saturation voltage calculation. V_{sg} is limited to then pinch-off voltage of (11), with a log-exp form, and this gives a current in subthreshold operation that varies exponentially with gate bias (lowly doped well resistors, that have a low JFET threshold voltage, in high voltage processes can be biased below threshold).

Although not detailed here, the model also includes self-heating modeling, and a separate contact resistance model. The contact resistance model includes a separate, implicit self-heating model based on (1), which allows the anomalous decrease in resistance with increasing current, seen in contacts to p -type material [7], to be modeled.

REFERENCES

- [1] C. C. McAndrew, "Predictive Technology Characterization, Missing Links Between TCAD and Compact Modeling," *Proc. IEEE SISPAD*, pp. 12-17, 2000.
- [2] R. V. H. Booth and C. C. McAndrew, "A 3-Terminal Model for Diffused and Ion-Implanted Resistors," *IEEE Trans. ED*, vol. 44, no. 5, pp. 809-814, May 1997.
- [3] C. C. McAndrew, S. Sekine, A. Cassagnes, and Z. Wu, "Physically-Based Effective Width Modeling of MOSFETs and Diffused Resistors," *Proc. IEEE ICMTS*, pp. 169-174, 2000.
- [4] F. N. Trofimenkoff, "Field-Dependent Mobility Analysis of the Field-Effect Transistor," *Proc. IEEE*, vol. 53, no. 11, pp. 1765-1766, Nov. 1965.
- [5] D. M. Caughey and R. E. Thomas, "Carrier Mobilities in Silicon Empirically Related to Doping and Fields," *Proc. IEEE*, vol. 55, no. 12, pp. 2192-2193, Dec. 1967.
- [6] C. C. McAndrew, "Useful Numerical techniques for Compact Modeling," *Proc. IEEE ICMTS*, pp. 121-126, 2002.
- [7] K. Banerjee, A. Amerasekera, G. Dixit and C. Hu, "Temperature and Current Effects on Small-Geometry-Contact Resistance," *Proc. IEEE IEDM*, pp. 115-118, 1997.